Solid Freeform Fabrication 2017: Proceedings of the 28th Annual International Solid Freeform Fabrication Symposium – An Additive Manufacturing Conference
Reviewed Paper

Fabrication of 3D Multi-material Parts Using Laser-based Powder Bed Fusion

C. Anstaett*, Dr.-Ing. C. Seidel*, Prof. Dr.-Ing G. Reinhart*
* Fraunhofer Research Institution for Casting, Composite and Processing Technology IGCV, Augsburg, Germany

Abstract

As different branches of industry use Laser Beam Melting (LBM) and more and more materials can be produced with it, this technology goes in and out of focus of production technologies in an industrial environment. A big advantage of LBM is the possibility of building very complex parts and therefore minimizing the need for raw material. The effects of this, such as lightweight-design, resource-efficient production and reduction of manufacturing time, can even be increased if material can be used locally defined in a part, so that one part does not have to consist of one material per fabrication-process, but at least two. Since LBM is a powder-bed-based process, the implementation of this idea is possible by adopting the conventional delivery device and the manufacturing process itself.
In this paper the results of a multi-material process are shown and the influences of different material properties on the manufacturing process are derived.

Introduction

In recent years multi-material has been in the scope of different research groups all over the world, especially in case of additive manufacturing. Thus far there are already ways to build multi-material parts out of plastic, using this technology for example, by using fused layer modeling (FDM) or stereolithography [1]. Also, in the case of parts made of metal, there are many approaches using laser powder depositioning, for example [2]. Even for powder-bed-based technologies there are many investigations being done concerning the powder depositioning [3–5, 5–7]. However, there is a big difference in the understanding of multi-material, especially in the case of laser beam based powder-bed fusion (LBM). They all have in common the combining of different materials, but vary in the way two or more materials are joined during the manufacturing process. In order to understand multi-material, Figure 1 shows the different kinds, as well as a mono-material part to more clearly point out the differences.

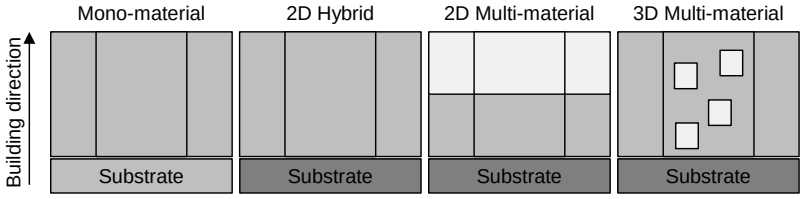

Figure 1: Parts categorized by the meaning of multi-material

A 2D Hybrid part differs from a mono-material part in the material of the substrate, which is the basis for the build-up process. While a mono-material process uses the same material for powder material as for the substrate, a 2D Hybrid process builds on a different material. It is also possible to use a conventionally manufactured part as substrate and start the additive building processes there. Hence, it is called a hybrid part, since different manufacturing techniques are used [8]. One example is shown by Fu et al. who built a copper-based alloy on a steel substrate [9]. One step further is to use LBM for production of both parts and build one material on top of the other. So a 2D Multi-material part can be produced, like Sing et al. has done [10]. This is called a 2D Multi-material part since the change of material occurs only in one dimension perpendicular to the building platform in direction of building. The highest level of multi-material parts consist of multiple materials distributed arbitrarily in the part in all dimensions – a 3D Multi-material part.

No matter what type of multi-material part is going to be built, the building process is influenced, since all materials vary in their material properties. Therefore the process parameters need to be adapted. A 3D Multi-material part has even more influence, since the process chain has to be modified in order to allocate and solidify different materials. In the next sections a methodical approach to build a 3D Multi-material part is shown using a copper-based alloy and tool steel 1.2709.

Experimental Setup

There are different approaches for integrating the second powder within the process in order to build a 3D Multi-material part [11]. An approach based on the conventional delivery device was used for this work, supplemented by a suction-module [3, 12, 13]. The process steps is shown in Figure **2**.

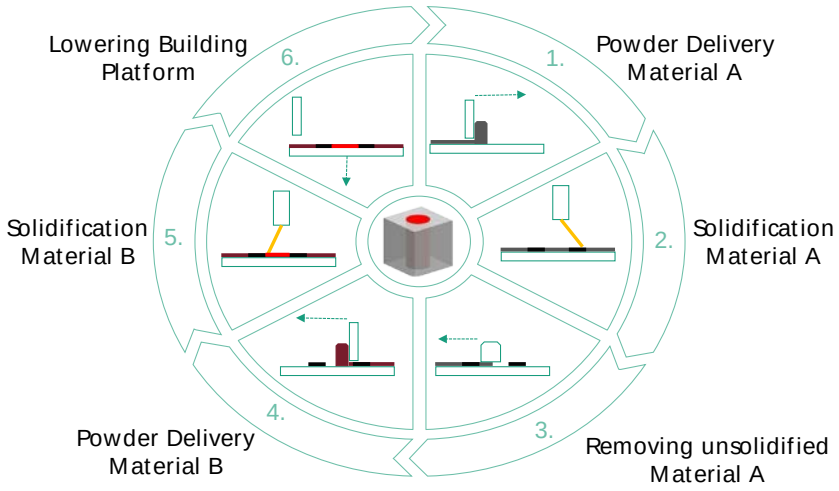

Figure 2: Process steps of the multi-material-LBM Process

After delivering and solidifying the material A, the non-solidified particles get removed via a suction-module. Afterwards the second powder of material B is delivered and solidified. This powder remains in the building chamber for the rest of the building process.

For this study an SLM 250HL machine from SLM Solutions was used. It is equipped with a fiber laser with a maximal power of 400 W and focal diameter of 100 µm. In addition, the following gas-atomized powder materials were utilized: Tool steel 1.2709 (X3NiCoMoTi18-9-5) [14] with a normal distribution between 10 and 45 µm, and 2.1293 CuCr1Zr (in the following called CCZ) [15], with a normal distribution between 20 and 45 µm. Both materials have a spherical shape. The chemical contribution of each material is shown in Table 1 and Table 2. Every sample was built with a layer thickness of 30 µm. The specimens were examined under a Nikon SMZ 1000 light microscope and a Keyence VK-9710 laser microscope. The density of the mono-material was tested using two different methods. First, the Archimedes method was used, which considers the entire specimen. Additionally, the porosity of polished samples was examined by microscopic analysis to get a comparability for the multi-material parts, which cannot be tested by the Archimedes method due to the unknown ratio of different materials [16, 17]. The material distribution within a 3D Multi-material part was measured with an EDX-System of Brucker Quantax 70 via a Hitatchi TM 3030 Plus scanning electron microscope.

Table 1 Chemical composition of 1.2709

C	Mo	Ni	Co	Ti	Fe
≤0.03	5.0	183.0	10.0	1.0	rest

Table 2 Chemical composition of CCZ

Cr	Zr	Fe	Si	other constituents	Cu
0.5-1.2	0.03-0.3	≤0.08	0.1	≤0.2	rest

Methodical Approach

In order to produce parts with a high density and to derive relationships and influences of the process, a methodical approach represented in Figure 3 was used.

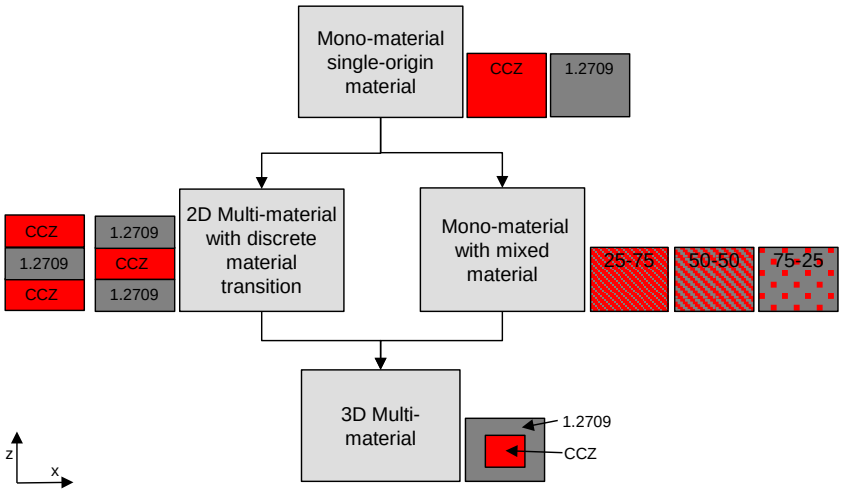

Figure 3: Methodical approach for building 3D Multi-material parts

First of all, the mono-materials are qualified for the LBM process. Based on existing publications for 1.2709 [7, 18] and CCZ [9, 19, 20], the proceeding promoted by [21] was used. However, as information already existed, building of single lines and areas was skipped and only the hatch spacing, scan speed and laser power were varied in the field of the presented parameters.

In a second step, parts with two 2D material transitions, which look like sandwich structures, are built to investigate the influence of different material properties on the transition area, e.g. the metallurgical appearance.

At the same time, parts with a mixture of both materials are produced to analyze the resulting material distribution and defining parameters for a transition area when building 3D multi-material parts. Here laser power and scanning speed are varied based on the evaluated mono-material-parameters, so that the resulting energy corresponds to the material distribution. There were three different mixing ratios under research, shown in Table 3.

Table 3 Mixing composition for building the mono-material parts with mixed powder

CCZ	1.2709
25%	75%
50%	50%
75%	25%

These parts will also be analyzed by EDX and later compared to results of the 3D Multi-material parts in order to analyze the composition of the overlap area.

Finally, the 3D Multi-material parts are built. Based on the knowledge gained from previous investigations and a pretest published at EuroPM 2017 [12], 3D Multi-material parts were built using the found parameters. The pretests have already shown that it is necessary to have an overlap between both material areas in order to build a connecting part [12]. Thus the following parts were all built using the found parameter sets and have an overlap of 0.2 mm (Figure 4, left). The focus of investigation is on the building order, the material solidification order and the cleanliness of each material area. In this case the building order means that the inner material – the core – or the surrounding material – the shell – is solidified first (Figure 4, right). The solidification order represents if 1.2709 or CCZ is first solidified. In the context of 3D Multi-material fabrication, cleanliness means alien particles of Material A within the area of Material B or vice-versa.

Figure 4**:** Left: Representation of overlap C between two different materials A and B; Right: Representation of building order in case of 3D Multi-material parts

Results and Discussion

Mono-material

Parameter analyses were performed and based on the need of high relative densities to reach good mechanical properties, the parameter set with the highest densities were used. Re-melting of the CCZ is necessary as a consequence of the limited laser power by 400 W and the goal of a good surface [12]. The parameter are shown in Figure **5**.

Table 4 Optimized parameters with density results from the Archimedes method [12]

Material	Hatch spacing (mm)	Scan speed (mm/s)	Laser power (W)	Re-melting	Relative density (%)
1.2709	0.105	600	200	No	100.00 ± 0.22
CCZ	0.125	600	400	Yes	99.28 ± 0.25

Figure 5 shows images of 1.2709 and CCZ made by a laser microscope. Both samples are produced using the mentioned parameters.

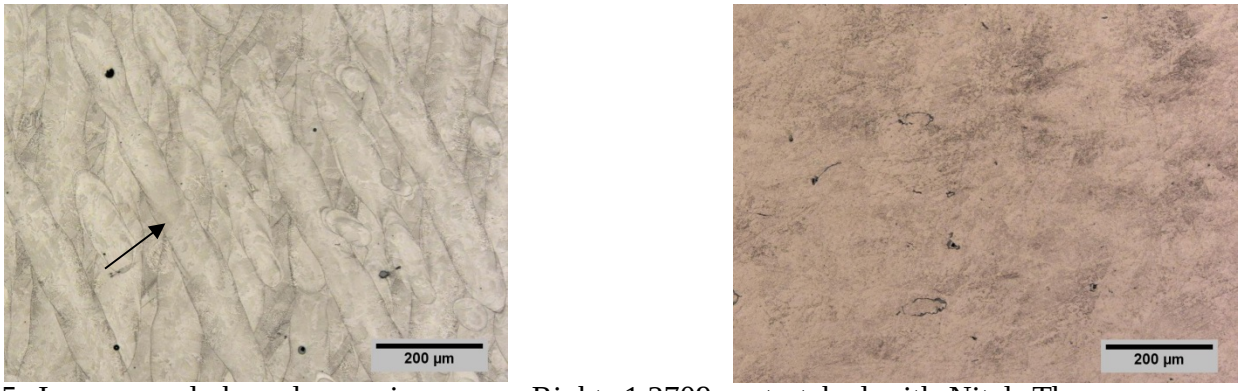

Figure 5: Images made by a laser microscope. Right: 1.2709 part etched with Nital. The arrow represents a melting line; Left: CCZ part etched with FeIIICl

While the image of the 1.2709 shows clear visible the melting lines, they are not visible in CCZ. This is due to the high heat conductivity of CCZ [15] and the re-melting strategy, which might cause a heat treatment-like process and therefore homogenizes the grain structure of the part.

2D Multi-material

During the manufacture of 2D Multi-material parts, the focus was on the transition areas. Figure **6** shows an overview of one part per building order as well as a magnification of each transition area.

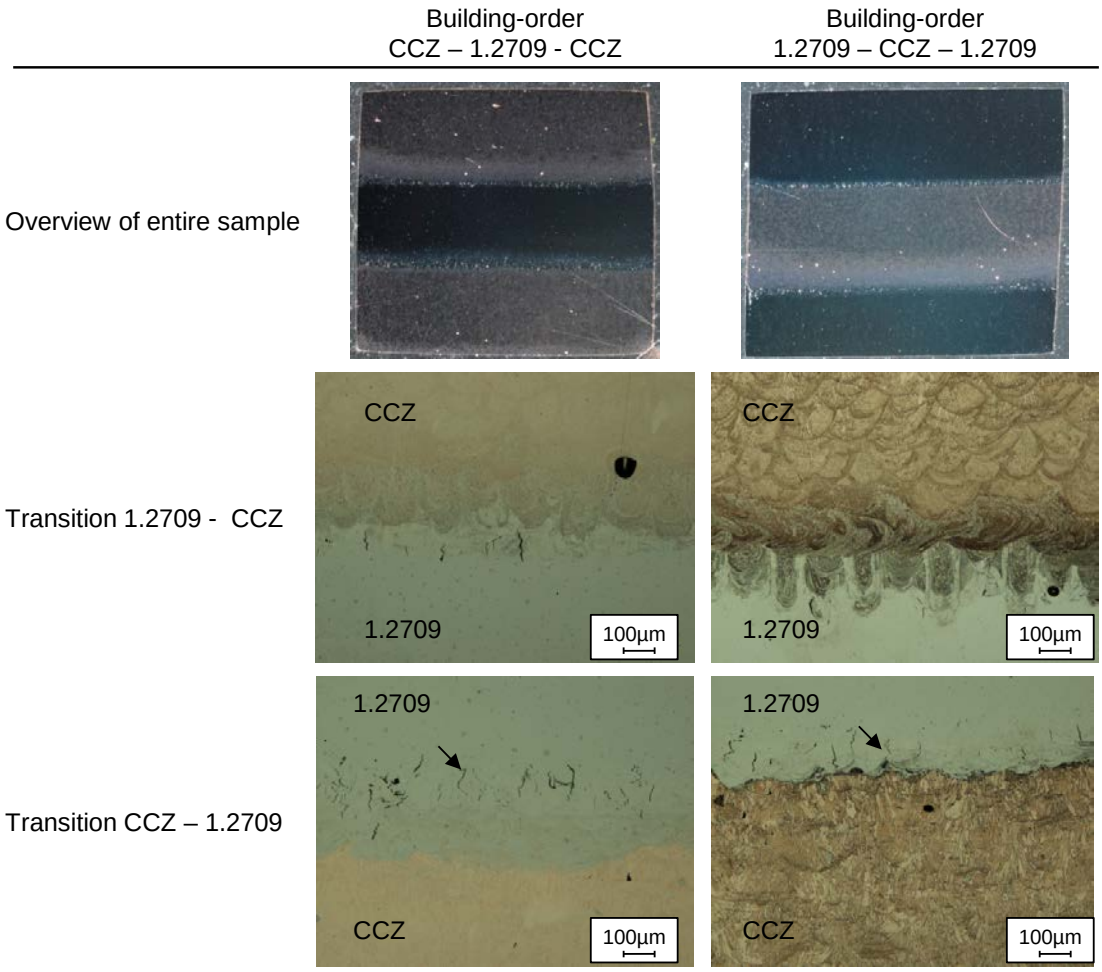

Figure 6: Images of sections of 2D Multi-material transitions in build-up direction. Pictures on the right for the transition area are etched. Arrows point at crack within the steel area. The images of the transition area of the building-order 1.2709 – CCZ – 1.2709 are etched.

The transition area for each kind of transition is similar in both building orders. In the case of CCZ-1.2709, it is stricter and there is almost no mixture of the materials. This is in contrast to what occurs for the transition of 1.2709-CCZ. This has already been found in the case of laser welding of copper and stainless steel by Chen et al. [22]. They called it a “fusion welding mode” if there is a mixture of melt as a consequence of both materials being briefly in a liquid phase and therefore able to mix up. As a consequence of both materials being in a liquid state, fewer cracks occur within this kind of building order, since the liquid copper is also able to fill up the cracks. This is equivalent to melting copper on top of steel. A “welding-brazing-mode” occurs only if the steel is liquid, representing the welding part of the joint, and the copper remains in a solid phase, representing the brazing part of the joint. For 2D Multi-material LBM this is equivalent to fusing steel on top of copper.

Focus on the etched images of the transition CCZ – 1.2709 shows melting lines in the copper area, although only in a small area above the transition. After this small area there are no more melting lines visible and the sample looks to the same as the images of the Mono-material process. In the 2D Multi-material process the differences in the thermal conductivity caused by the influence of 1.2709 might give the melting line more time for cooling and therefore make the melting lines visible.

Mono-material with mixed powder

By building parts with mixed powder the influence of the material on the parameter and the resulting material composition can be determined. The parameters were varied between the known set for the original powders represented in Table 4 corresponding to the material mixture. The parameters with the best relative densities are shown in Table 5.

Table 5 Parameters and relative density of samples with mixed powder

Material 1.2709 (%)	CCZ (%)	Hatch spacing (mm)	Scan speed (mm/s)	Laser power (W)	Re-melting	Relative density (%)
25	75	0,115	600	300	No	99,96
50	50	0,118	600	333	No	99,98
75	25	0,125	600	400	Yes	99,99

It can be seen that the parameters vary from the single-origin parameters because of the different material properties. However, there is a bigger influence of the CCZ than the 1.2709, since the parameters, and therefore the fed energy, tends to be more similar to the parameters of CCZ.

3D Multi-material

The following Figure 7 shows 3D Multi-material samples built with different building-order and solidification-order.

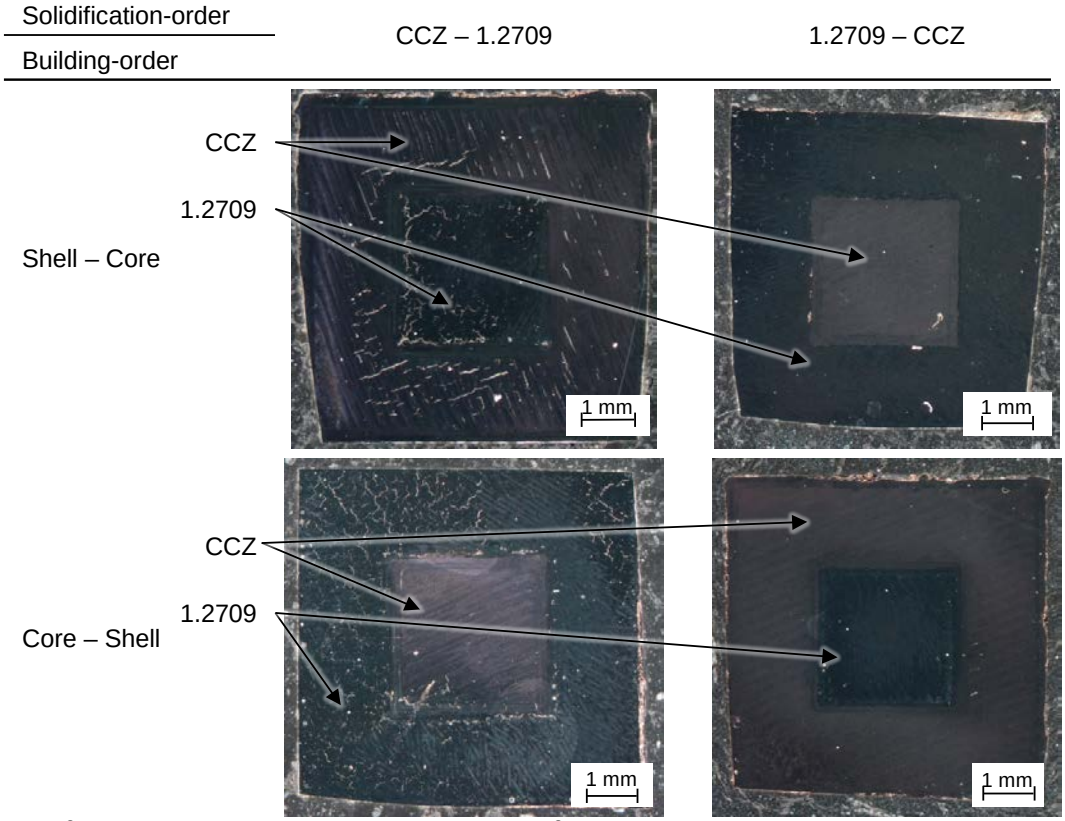

Figure 7**:** Images of polished samples with varying solidification- and building-order

There are visible differences in the quality of the parts depending on the solidification-order but no influences of the building-order. Since many cracks occur in the shell while first solidifying CCZ, this does not happen when 1.2709 is the first material solidified. There can be two reasons for this. First, corresponding to the results from the 2D Multi-material parts and from Chen et al. [22], both materials are in a solid phase while merging and therefore internal stresses in the material are reduced, if CCZ is solidifying second. The other possibility for the absence of cracks is that alien particles act as a source for cracks. That is why EDX-analyses were performed to analyze the distribution of Fe and Cu within the samples. These two elements were chosen since they represent the main part of each material. Results are shown in Figure 8.

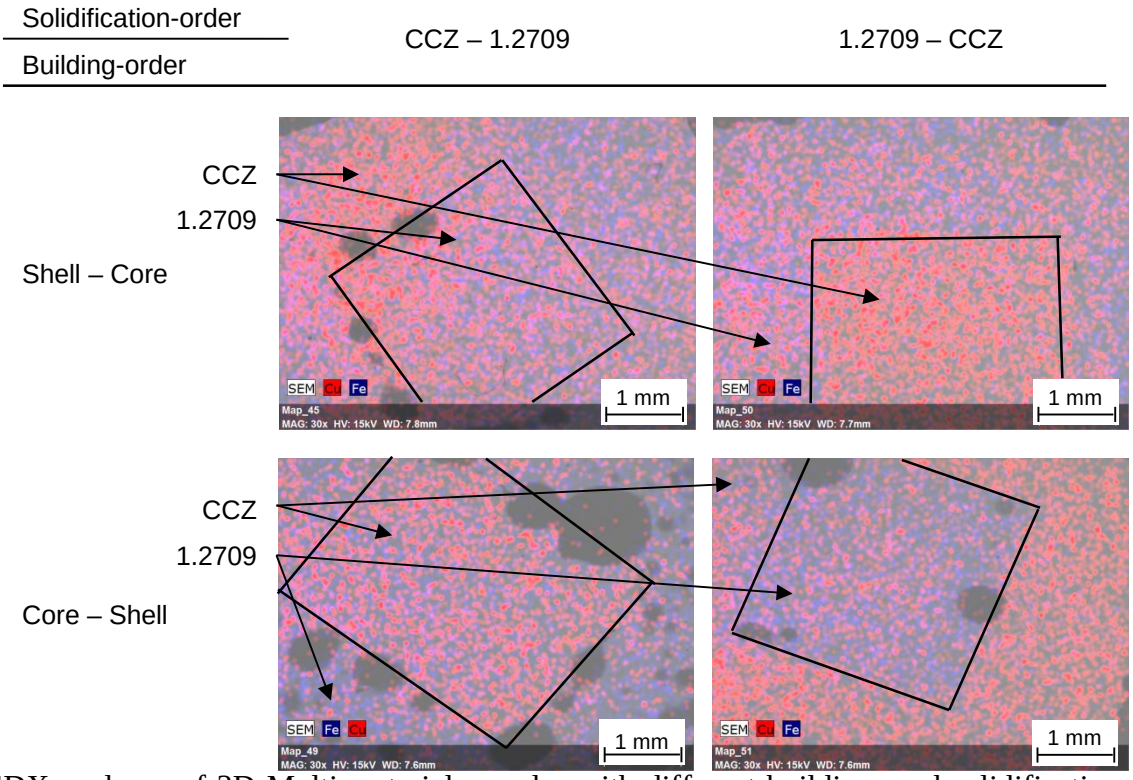

Figure 8**:** EDX analyses of 3D Multi-material samples with different building- and solidification order. Fe is shown in blue and Cu in red: The black squares show the area of the core

It can be seen that the 1.2709-powder can be removed more easily than the CCZ, since all images contain traces of Cu, while Fe is only in the area where it should remain – especially if this powder is delivered first. This supports the assumption that Fe-particles within the CCZ-part support the formation of cracks, since they might not become molten properly and therefore remain solid.

It is conspicuous that in all cases the second delivered material is distributed over the entire sample. This can occur since the roughness of the first solidified material is too high and the second delivered powder fills up the gaps. The other possibility is that the first solidified material shrinks while solidifying [23] and the difference to the expected layer thickness gets filled up. In this case the cross-contamination will increase as the height of the part increases. However, both assumptions will be analyzed in future investigations.

Conclusion and Outlook

A methodical approach was presented showing the procedure for building a 3D Multi-material part. After qualifying the CCZ and 1.2709 for the Mono-material process and therefore are able to build parts with a higher relative density of 99.5%. In a next step 2D Mutli-material parts were built showing the influence of the solidification-order on forming cracks in the steel. In the case of building CCZ on top of 1.2709 the quantity of cracks is decreased, since both materials are in liquid phase when CCZ becomes molten, since it requires more energy for melting, which leads to a mixture of both materials. The building of parts with mixed powder showed the influence of alien particles within the base material, since each mixture requires a different set of parameters for building parts with a high rel. density. In future investigations this set of parameters will be used for the transition area to build parts with a specific material distribution in this area. In a final step, 3D Mutli-material parts were built using the parameters from the Mono-material process. Depending on the solidification-order, the cracks occurred within the steel area for the same reason as they did within the 2D Multi-material parts. Alien particles, especially of CCZ, were found within the other area by using EDX analyses. Two possible reasons – the shrinkage of the melting pool and the roughness of the first delivered material – will be investigated in future research.

Acknowledgements

The authors want to thank the Bavarian Research Foundation for the financial support within the project ForNextGen.

References

[1] J.-W. Choi, H.-C. Kim, R. Wicker, Multi-material stereolithography, Journal of Materials Processing Technology 211 (2011) 318–328.
[2] P. Muller, P. Mognol, J.-Y. Hascoet, Modeling and control of a direct laser powder deposition process for Functionally Graded Materials (FGM) parts manufacturing, Journal of Materials Processing Technology 213 (2013) 685–692.
[3] Y. Chivel, New Approach to Multi-material Processing in Selective Laser Melting, Physics Procedia 83 (2016) 891–898.
[4] C. Andriani, K.C. Chua, H.Z. Liu, Review on Melting of Multiple Metal Materials in Additive Manufacturing, in: C.C. Kai, Y.W. Yee, T.M. Jen, L. Erjia (Eds.), Proceedings of the 1st International Conference on Progress in Additive Manufacturing, Research Publishing Services, Singapore, 2014, pp. 170–175.
[5] P. Kumar, E. Beck, S. Das, Preliminary Investigations on the Deposition of fine Powders through Miniature Hopper-Nozzles Applied to Multi-Material Solid Freeform Fabrication, SFF-Symposium (2003).
[6] A.V. Kumar, A. Dutta, J.E. Fay, Electrophotographic printing of part and binder powders, Rapid Prototyping Journal 10 (2004) 7–13.
[7] M. Ott, Multimaterialverarbeitung bei der additiven strahl- und pulverbettbasierten Fertigung, Herbert Utz Verlag, München, 2012.
[8] Danielle Strong, Issariya Sirichakwal, Guha P. Manogharan and Thomas Wakefield, Current state and potential of additive - hybrid manufacturing for metal parts.
[9] T.C. Fu, W.Y. Yeong, S. Chen, Selective laser melting of copper based alloy on Steel: A Preliminiary Study.
[10] S.L. Sing, L.P. Lam, D.Q. Zhang, Z.H. Liu, C.K. Chua, Interfacial characterization of SLM parts in multi-material processing: Intermetallic phase formation between AlSi10Mg and C18400 copper alloy, Materials Characterization 107 (2015) 220–227.
[11] C. Anstaett, C. Seidel, G. Reinhart, Mutli-Material Processing Laser Beam Melting, Fraunhofer Direct Digital Manufacturing Conference (2016).
[12] C. Anstaett, M. Schafnitz, C. Seidel, G. Reinhart, Laser-Based Powder Bed-Fusion of 3D-Multi-Material-Parts of Copper-Chrom-Zirconia And Tool Stee, European Powder Metallurgy Association Proceedings (2017).
[13] Yuri Alexandrovich Chivel, Igor Smurov, Bernard Laget, Igor Yadroitsev, EP20090167817 (2010).
[14] Deutsche Ingenieurs Norm, Werkstoffdatenblatt 1.2709.
[15] Deutsches Kupferinstitut, Werkstoffdatenbaltt CuCrZr (2005).
[16] A.B. Spierings, M. Schneider, R. Eggenberger, Comparison of density measurement techniques for additive manufactured metallic parts, Rapid Prototyping Journal 17 (2011) 380–386.
[17] W.W. Wits, S. Carmignato, F. Zanini, T.H. Vaneker, Porosity testing methods for the quality assessment of selective laser melted parts, CIRP Annals - Manufacturing Technology 65 (2016) 201–204.
[18] J. Bräunig, T. Töppel, B. Müller, M. Burkhardt, T. Hipke, W.-G. Drossel, Advanced Material Studies for Additive Manufacturing in terms of Future Gear Application, Advances in Mechanical Engineering 6 (2014) 741083.
[19] D. Becker, Selektives Laserschmelzen von Kupfer und Kupferlegierungen. Zugl.: Aachen, Techn. Hochsch., Diss., 2014, first. Aufl., Apprimus-Verl., Aachen, 2014.
[20] E. Uhlmann, Tekkaya, A.E. Kashevko, V., S. Gles, R. Reimann, P. John, Qualification of CuCr1Zr for the SLM Process, 7th International Conference on High Speed Forming (2016).
[21] I. Yadroitsev, P. Krakhmalev, I. Yadroitsava, Hierarchical design principles of selective laser melting for high quality metallic objects, Additive Manufacturing 7 (2015) 45–56.
[22] S. Chen, J. Huang, J. Xia, H. Zhang, X. Zhao, Microstructural Characteristics of a Stainless Steel/Copper Dissimilar Joint Made by Laser Welding, Metall and Mat Trans A 44 (2013) 3690–3696.

[23] A.B. Spierings, G. Levy, Comparison of density of stainless steel 316L parts produced with selective laser melting using different powder grades, Solid Feeform Fabrication Proceedings (2009).